ACCSCIENCE PUBLISHING

Eurasian Journal of Medicine and Oncology

ORIGINAL RESEARCH ARTICLE

Regulation of X-linked inhibitor of apoptosis protein by androgen deprivation therapy promotes castration-resistant prostate cancer progression

Ke Ren*, Xin Gou, and Weiyang He

Department of Urology, The First Affiliated Hospital of Chongqing Medical University, Chongqing, China

Abstract

Introduction: Hormone-sensitive prostate cancer typically progresses to a castration-resistant stage after an average of 18–24 months of androgen deprivation therapy (ADT). The anti-apoptotic factor X-linked inhibitor of apoptosis protein (XIAP) is not only implicated in the development of prostate cancer but also plays a critical role in its progression to the castration-resistant state.

Objective: This study aims to investigate the relationship between ADT and the regulation of XIAP.

Methods: The protein expression levels of midline 1 (MID1), serine/threonine kinase proviral integration site for Moloney murine leukemia virus 2 (PIM2), protein phosphatase 2A (PP2A), eukaryotic translation initiation factor 4B (EIF4B), phosphorylated EIF4B, and XIAP were analyzed and compared among castration-naïve, hormone-sensitive, and castration-resistant prostate cancer (CRPC) tissues. The *MID1* gene was manipulated in both androgen-dependent and androgen-independent prostate cancer cells to evaluate its effect on XIAP protein expression and the apoptosis rate of the prostate cancer cells.

Results: XIAP protein expression and EIF4B phosphorylation levels were significantly increased in CRPC. In contrast, PIM2 and EIF4B protein expression levels remained similar before and after the development of castration resistance. MID1 protein expression level was significantly elevated, while PP2A expression was significantly reduced in CRPC tissues.

Conclusion: ADT may lead to elevated MID1 and reduced PP2A protein expression levels, which indirectly enhance the phosphorylation activity of PIM2 on EIF4B, thereby increasing XIAP expression and reducing apoptosis in prostate cancer cells. This mechanism likely contributes to disease progression toward the castration-resistant stage.

Keywords: Androgen deprivation therapy; Apoptosis; Castration-resistant prostate cancer; X-linked inhibitor of apoptosis protein

***Corresponding author:**
Ke Ren
(203020@cqmu.edu.cn)

Citation: Ren K, Gou X, He W. Regulation of X-linked inhibitor of apoptosis protein by androgen deprivation therapy promotes castration-resistant prostate cancer progression. *Eurasian J Med Oncol.* 2026;10(1):162-172. doi: 10.36922/EJMO025160127

Received: April 17, 2025

1st revised: May 31, 2025

2nd revised: June 21, 2025

Accepted: July 1, 2025

Published online: August 5, 2025

1. Introduction

Prostate cancer is an androgen-dependent malignant tumor, and inhibition of the androgen receptor (AR) signaling pathway can suppress tumor growth and progression.

Androgen deprivation therapy (ADT) is one of the most fundamental treatment methods for inhibiting the AR signaling pathway and serves as the foundation of all drug-based treatments for advanced prostate cancer. ADT effectively suppresses tumor proliferation during the hormone-sensitive stage; however, it cannot prevent the progression of prostate cancer to a castration-resistant stage.[1] After an average of 18–24 months of ADT treatment, nearly all hormone-sensitive prostate cancers (HSPCs) progress to the castration-resistant stage, in which ADT alone is no longer sufficient to control tumor growth. The disease then progresses more rapidly, posing a greater threat to the patient's life and making treatment more challenging. Although the specific mechanisms underlying castration resistance in prostate cancer remain unclear, clinical observations suggest that delaying ADT initiation may postpone the onset of castration resistance. Moreover, compared with traditional continuous ADT, intermittent ADT has been reported to delay, to some extent, the progression to castration-resistant prostate cancer (CRPC).[2,3] These findings imply a potential relationship between ADT and the development of castration resistance.

The serine/threonine kinase proviral integration site for Moloney murine leukemia virus 2 (PIM2) is aberrantly overexpressed in prostate cancer cells.[4] PIM2 phosphorylates eukaryotic translation initiation factor 4B (EIF4B) at Ser422, thereby promoting the translation of the downstream anti-apoptotic factor X-linked inhibitor of apoptosis protein (XIAP).[5] Thus, the PIM2/EIF4B/XIAP signaling pathway has been shown to effectively inhibit apoptosis in prostate cancer cells and contribute to disease progression.

As the most potent anti-apoptotic factor in its family, XIAP is not only involved in the tumorigenesis of multiple malignancies but has also been shown to be associated with accelerated progression and poor prognosis in several cancer types. For example, melanoma and ovarian cancer cells with high XIAP expression are more invasive; esophageal cancer cells with elevated XIAP expression are less sensitive to chemotherapeutic agents; renal cell carcinoma cells with increased XIAP expression are more likely to metastasize; and liver cancer cells with high XIAP expression are more prone to post-operative recurrence.[6-9] CRPC represents an advanced stage of prostate cancer and shares biological characteristics with other malignancies exhibiting elevated XIAP expression. In addition, XIAP has been reported as a predictive marker for CRPC.[10] Therefore, XIAP is considered to be associated with the progression to CRPC. However, the regulatory mechanism of XIAP during the transition from HSPC to CRPC remains unclear.

This study aims to explore the influence of ADT on castration-resistant progression through modulation of XIAP expression.

2. Materials and methods

2.1. Materials

Androgen-dependent prostate cancer cell line LNCaP and androgen-independent prostate cancer cell line PC-3 were purchased from American Type Culture Collection (ATCC), United States of America (USA). Lipofectamine™ reagent was purchased from Invitrogen, USA. Antibodies for protein phosphatase 2A (PP2A; sc-80662), PIM2 (sc-13674), EIF4B (sc-376062), and XIAP (sc-55550) were purchased from Santa Cruz Biotechnology, USA. Antibody for phosphorylated EIF4B (p-EIF4B) (Ser-422) was purchased from Cell Signaling Technology, USA. Antibody for midline 1 (MID1; ab70770) was purchased from Abcam, China. M-PER™ Mammalian Protein Extraction Reagent and SuperSignal West Pico Chemiluminescent Substrate were purchased from Pierce, USA. Taxotere® cytotoxic agent docetaxel was purchased from Sanofi, France.

2.2. Clinical sample collection

From March 2014 to December 2020, 11 patients initially diagnosed with metastatic prostate cancer at the First Affiliated Hospital of Chongqing Medical University, Chongqing, China – who underwent continuous ADT and eventually progressed to metastatic CRPC (mCRPC) – were enrolled in this study (group A). Prostate cancer samples from initial prostate biopsy (castration-naïve stage) were collected. In addition, all 11 patients developed severe local symptoms such as urinary obstruction or bleeding after progression to mCRPC, and subsequently underwent transurethral resection; prostate cancer samples from the castration-resistant stage were also collected. During the same period, 38 patients initially diagnosed with locally advanced prostate cancer (cT3b-T4) at the same hospital – who underwent radical prostatectomy following neoadjuvant ADT – were also included.

The neoadjuvant ADT regimen (goserelin or triptorelin combined with bicalutamide) was administered for 1–3 months in 16 patients (group B), 6–9 months in 13 patients (group C), and 12 months or more in nine patients (group D). For each patient, prostate cancer samples from both the initial prostate biopsy (castration-naïve stage) and radical prostatectomy (hormone-sensitive stage) were collected. The baseline characteristics of the four patient groups are summarized in Table 1.

All clinical specimens were pathologically confirmed to be prostatic adenocarcinoma, with positive prostate-specific antigen (PSA) and AR expression. Cases

Table 1. Baseline characteristics of the patients

Baseline characteristics of the patients	Group A (%)	Group B (%)	Group C (%)	Group D (%)
Number of cases	11	16	13	9
Mean age (years)	69 (58–81)	67 (53–76)	71 (49–78)	65 (59–76)
Initial protein-specific antigen (ng/mL)				
<10	0 (0)	2 (12.5)	1 (7.7)	0 (0)
10–20	2 (18.2)	6 (37.5)	4 (30.8)	1 (11.1)
>20	9 (81.8)	8 (50.0)	8 (61.5)	8 (88.9)
Gleason score				
≤6	1 (9.1)	0 (0)	0 (0)	1 (11.1)
7	6 (54.5)	10 (62.5)	8 (61.5)	5 (55.6)
≥8	4 (36.4)	6 (37.5)	5 (38.5)	3 (33.3)
Clinical stage				
T3bN0M0	0 (0)	9 (56.3)	4 (30.8)	0 (0)
T4N0M0	0 (0)	2 (12.5)	4 (30.8)	2 (22.2)
T3b-4N1M0	0 (0)	5 (31.2)	5 (38.4)	7 (77.8)
TxNxM1b	11 (100%)	0 (0)	0 (0)	0 (0)

Abbreviations: N: Node; M: Metastasis; T: Tumor.

exhibiting neuroendocrine differentiation or intraductal carcinoma components were excluded. Each tissue sample was divided equally into two parts: One part was preserved in formalin for pathological examination, and the other was preserved in liquid nitrogen for protein detection.

2.3. Cell culture, transfection, and RNA interference

The androgen-dependent prostate cancer cell line (LNCaP) and the androgen-independent prostate cancer cell line (PC-3) were purchased from the ATCC. RPMI-1640 complete medium (9 mL RPMI-1640 + 1 mL fetal bovine serum [FBS] + 100 Ml 1% penicillin/streptomycin) was used for cell culture under 5% CO_2 at 37°C. To simulate androgen deprivation *in vitro*, prostate cancer cells were cultured in medium supplemented with charcoal/dextran-treated steroid-free FBS.[10]

The *MID1* gene was transfected into LNCaP cells to increase its expression. The short form of human *MID1* cDNA was cloned from a cDNA library by reverse transcription-polymerase chain reaction using the following primers: sense, 5'-GCCAGTTTTGTGACCAGGAT-3'; antisense: 5'-ATGTGAGAGTCCGGAATTGG-3.'

Restriction enzyme sites for EcoRI and SalI were introduced at the 5' ends of the sense and antisense primers, respectively. The cDNA was inserted into the mammalian expression plasmid pCI-neo, and the plasmid was fully sequenced to verify the accuracy of the cloning process. Lipofectamine™ reagent was used for the transfection. Cells that survived in Dulbecco's Modified Eagle Medium containing neomycin (400 μg/mL) were considered LNCaP/*MID1 cells*.

Expression of *MID1* in PC-3 cells was silenced by *MID1* small interfering RNA (siRNA) transfection. A *MID1*-specific RNA interference eukaryotic expression vector, pGenesil-1, was constructed. The siRNA sequence was designed with the following structure: BamHI–sense DNA–loop (TCAAGAG)–antisense DNA–stop codon–HindIII. The sense strand sequence was 5'-GGCATGGAAACACTGGAGTCA-3.' Lipofectamine™ reagent was also used for siRNA transfection. The silencing efficiency was verified by Western blot analysis.

2.4. Western blot

M-PER™ Mammalian Protein Extraction Reagent was used to extract total protein from cell lysates and tissue homogenates. Protein concentrations (5 μg/μL for cell lysates and 10 μg/μL for tissue lysates) were determined using the Bradford assay (Bio-Rad, USA). A total of 10 μL of protein sample mixed with ×1 loading buffer was loaded and separated on a 10% sodium dodecyl sulfate polyacrylamide gel electrophoresis. Proteins were transferred to a polyvinylidene fluoride membrane in a transfer buffer (25 mM Tris, 0.2 M glycine, 20% methanol) at 400 mA for 1 h. The membrane was blocked at room temperature for 1 h in Tris-buffered saline with 0.1% Tween-20 containing 7% skimmed milk powder.

Primary antibodies were diluted according to the manufacturer's protocol as follows: MID1 (1:800), PP2A (1:800), PIM2 (1:800), EIF4B (1:1000), p-EIF4B (1:1000), XIAP (1:800), and glyceraldehyde-3-phosphate dehydrogenase (1:400). After incubation with appropriately diluted horseradish peroxidase-conjugated secondary antibodies, detection was performed using the SuperSignal™ West Pico Chemiluminescent Substrate with an exposure time of 30 s. Finally, the films were developed and scanned using an Epson scanner (Epson Expression 1640XL, Epson, Japan).

2.5. Cell apoptosis rate analysis

The cytotoxic agent docetaxel was added to the culture medium at a concentration of 100 nM. Cells were collected at the logarithmic growth phase after 72 h of treatment, and the concentration was adjusted to 10^6 cells/mL. After centrifugation at 1,000 rpm for 5 min, 100 μL of ×1 binding buffer was added for resuspension. Subsequently, 5 μL of Annexin V-FITC and 10 μL of propidium iodide were added. The samples were then incubated in the dark at room temperature for 20 min, followed by the addition

of 400 µL of ×1 binding buffer. Apoptosis rates were analyzed using flow cytometry (ZE5 Cell Analyzer, Agilent Technologies, USA). Data were further analyzed using FACScan software (BD Biosciences, USA). The apoptosis rate was defined as the ratio of apoptotic cells to the total number of cells. Each experimental group was assessed in triplicate, and the mean value was calculated.

2.6. Statistics

Data were expressed as mean ± standard deviation and analyzed using the Statistical Package for the Social Sciences version 19.0 (IBM, USA). Student's *t*-test was employed for comparisons between two groups, whereas one-way analysis of variance was used to compare means among multiple groups. $p<0.05$ was considered statistically significant.

3. Results

3.1. PP2A competes with PIM2 for EIF4B phosphorylation in CRPC

For each patient in group A, the protein expression of the anti-apoptotic factor XIAP in prostate cancer samples at the castration-naïve stage was compared with that at the castration-resistant stage. XIAP was expressed at both stages but was significantly higher at the castration-resistant stage, regardless of the Gleason score (Figure 1). Based on previous findings indicating that XIAP expression in prostate cancer is regulated by PIM2 and the phosphorylation level of its downstream substrate EIF4B, the protein expression levels of PIM2, EIF4B, and p-EIF4B were compared in prostate cancer samples obtained before and after the development of castration resistance. The results revealed that the p-EIF4B level was significantly higher at the castration-resistant stage compared to the castration-naïve stage, regardless of Gleason score, demonstrating a similar trend to that of XIAP. However, no significant differences were observed in the protein levels of PIM2 and EIF4B between the two stages (Figure 2), which does not account for the observed differences in p-EIF4B levels. Previous research indicated that EIF4B phosphorylation is primarily regulated by PIM2. Therefore, additional factors are likely involved in modulating EIF4B phosphorylation during the progression to castration resistance.

As an enzyme with dephosphorylating activity that counteracts the phosphorylation effect of kinase, PP2A has been reported to be associated with the dephosphorylation of p-EIF4B. Therefore, the protein expression levels of PP2A and MID1, a protein involved in modulating PP2A activity, were analyzed in prostate cancer samples obtained before and after the development of castration resistance. The findings revealed that PP2A expression was significantly lower after castration resistance, whereas MID1 expression was significantly higher, regardless of the Gleason score (Figure 3).

3.2. ADT activates the MID1/PP2A/p-EIF4B/XIAP signaling pathway in prostate cancer

For patients in group B who underwent 1–3 months of neoadjuvant ADT, the protein expression levels of XIAP were similar before and after castration in cases with a Gleason score of <7. However, in cases with a Gleason score of 8–10, XIAP levels were significantly elevated after castration. The protein expression levels of p-EIF4B demonstrated a similar trend to XIAP. Both PIM2 and EIF4B protein expression levels were similar before and after castration, regardless of Gleason score. Even in cases with a Gleason score of 8–10, no significant differences

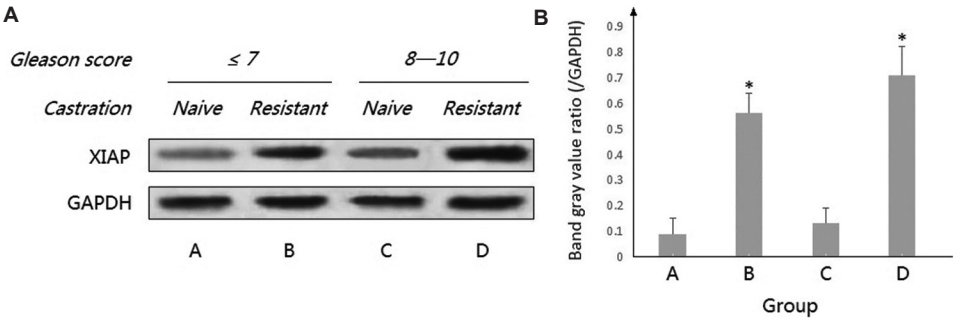

Figure 1. XIAP expression in metastatic prostate cancer tissues. (A) Western blot results; (B) Quantification of XIAP protein expression based on the band intensity ratio of XIAP to GAPDH. In patients with a Gleason score ≤7 ($n = 7$), XIAP protein expression levels were 0.092 ± 0.075 a.u. at the mHSPC stage (group A) and 0.563 ± 0.098 a.u. at the mCRPC stage (group B), showing a statistically significant difference between groups A and B. In patients with a Gleason score of 8–10 ($n = 4$), XIAP protein expression levels were 0.130 ± 0.071 a.u. at the mHSPC stage (group C) and 0.712 ± 0.112 a.u. at the mCRPC stage (group D), also demonstrating a significant difference between groups A and D.
Note: Asterisk (*) indicates statistical significance at $p<0.05$
Abbreviations: a.u.: Arbitrary units; GAPDH: Glyceraldehyde-3-phosphate dehydrogenase; mCRPC: Metastatic castration-resistant prostate cancer; mHSPC: Metastatic hormone-sensitive prostate cancer; XIAP: X-linked inhibitor of apoptosis protein.

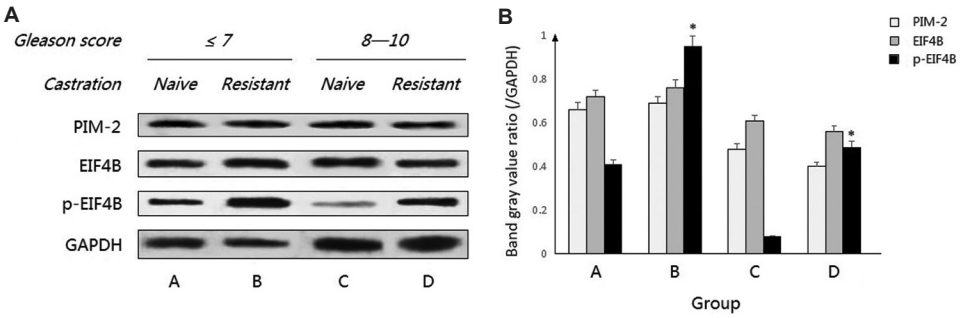

Figure 2. The expression of PIM2, EIF4B, and p-EIF4B in metastatic prostate cancer tissues. (A) Western blot results; (B) Quantification of protein expression levels based on the band intensity ratio of each target protein to GAPDH. In patients with a Gleason score ≤7 (n = 7), p-EIF4B protein expression levels were 0.412 ± 0.029 a.u. at the mHSPC stage (group A) and 0.956 ± 0.043 a.u. at the mCRPC stage (group B), indicating a statistically significant difference between groups A and B. However, for PIM2 and EIF4B, no significant differences were observed between groups A and B. In patients with a Gleason score of 8–10 (n = 4), p-EIF4B protein expression levels were 0.081 ± 0.007 a.u. at the mHSPC stage (group C) and 0.495 ± 0.137 a.u. at the mCRPC stage (group D), demonstrating a statistically significant difference between groups C and D. However, for PIM2 and EIF4B, no significant differences were observed between groups C and D.

Note: Asterisk (*) indicates statistical significance at p<0.05

Abbreviations: a.u.: Arbitrary units; EIF4B: Eukaryotic translation initiation factor 4B; GAPDH: Glyceraldehyde-3-phosphate dehydrogenase; mCRPC: Metastatic castration-resistant prostate cancer; mHSPC: Metastatic hormone-sensitive prostate cancer; p-EIF4B: Phosphorylated eukaryotic translation initiation factor 4B; PIM2: Proviral integration site for Moloney murine leukemia virus 2.

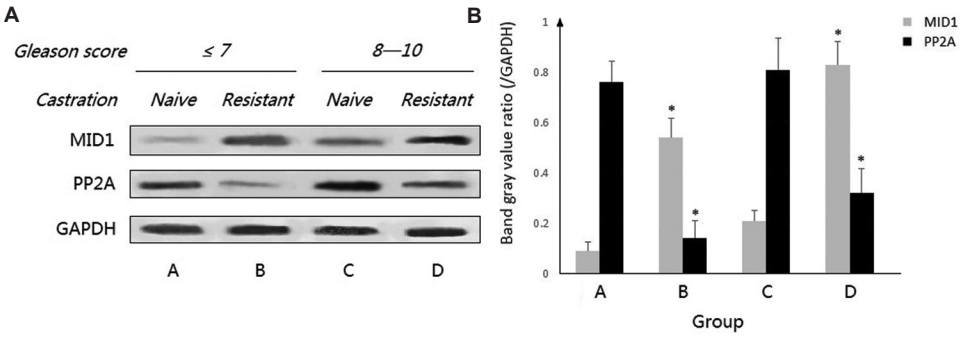

Figure 3. The expression of MID1 and PP2A in metastatic prostate cancer tissues. (A) Western blot results; (B) Quantification of protein expression levels based on the band intensity ratio of each target protein to GAPDH. In patients with a Gleason score ≤7 (n = 7), MID1 protein expression levels were 0.091 ± 0.043 a.u. at the mHSPC stage (group A) and 0.540 ± 0.098 a.u. at the mCRPC stage (group B), indicating a statistically significant difference between groups A and B. PP2A protein expression levels were 0.763 ± 0.116 a.u. at the mHSPC stage (group A) and 0.141 ± 0.082 a.u. at the mCRPC stage (group), demonstrating a statistically significant difference between groups A and B. In patients with a Gleason score of 8–10 (n = 4), MID1 and PP2A protein expression levels exhibited trends similar to those observed in patients with a Gleason score ≤7.

Note: Asterisk (*) indicates statistical significance at p<0.05.

Abbreviations: a.u.: Arbitrary units; GAPDH: Glyceraldehyde-3-phosphate dehydrogenase; MID1: Midline 1; PP2A: Protein phosphatase 2A

were observed in PIM2 and EIF4B protein expression levels before and after castration. In addition, PP2A protein expression levels were significantly lower after castration in cases with a Gleason score of 8–10, but not in those with a Gleason score <8. Moreover, MID1 protein expression levels were significantly elevated after castration in cases with a Gleason score of 8–10, but not in those with a Gleason score <8 (Figure 4).

For patients in group C who underwent 6–9 months of neoadjuvant ADT, XIAP protein expression levels were significantly elevated after castration, regardless of the Gleason score. Predictably, the trend of p-EIF4B levels in each group was entirely consistent with that of XIAP. Both PIM2 and EIF4B protein expression levels were similar before and after castration, regardless of the Gleason score. PP2A protein expression levels were significantly lower after castration, whereas MID1 protein expression levels were significantly higher, regardless of the Gleason score (Figure 5).

For patients in group D who underwent at least 12 months of neoadjuvant ADT, the expression levels of each target factor – including XIAP, p-EIF4B, EIF4B, PIM2, PP2A, and MID1–before and after castration followed exactly the same trends as those observed in group C (Figure 6).

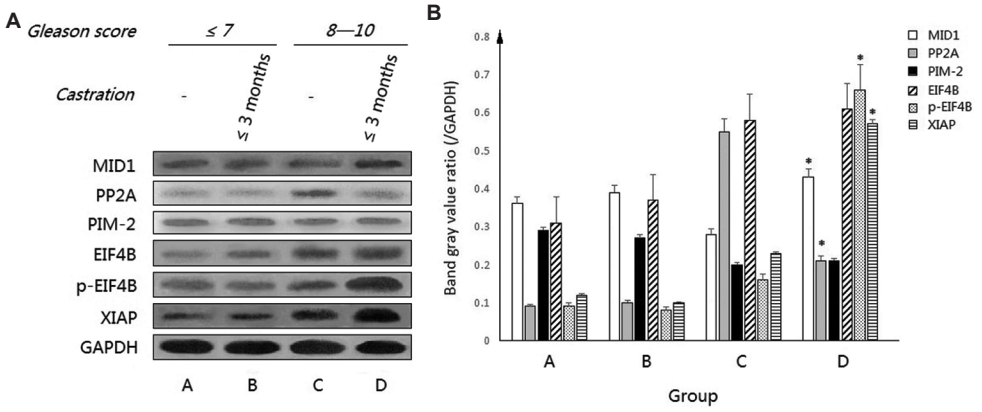

Figure 4. Expression of target proteins in patients with prostate cancer receiving no more than 3 months of neoadjuvant ADT (group B; n = 16). (A) Western blot results; (B) Quantification of protein expression levels based on the band intensity ratio of each target protein to GAPDH. In patients with a Gleason score ≤7 (n = 10), no significant differences were observed in the protein expression levels of XIAP, p-EIF4B, PIM2, EIF4B, MID1, and PP2A before and after ADT (groups A vs. group B). In patients with a Gleason score of 8–10 (n = 6), XIAP protein expression levels were 0.232 ± 0.009 a.u. before ADT (group C) and 0.570 ± 0.146 a.u. after ADT (group D), demonstrating a statistically significant difference between groups C and D. The protein expression levels of p-EIF4B were 0.161 ± 0.011 a.u. before ADT (group C) and 0.662 ± 0.074 a.u. after ADT (group D), indicating a statistically significant difference between groups C and D. MID1 protein expression levels were 0.280 ± 0.014 a.u. before ADT (group C) and 0.432 ± 0.027 a.u. after ADT (group D), demonstrating a statistically significant difference between groups C and D. The protein expression levels of PP2A were 0.553 ± 0.029 a.u. before ADT (group C) and 0.212 ± 0.015 a.u. after ADT (group D), indicating a statistically significant difference between groups C and D. For PIM2 and EIF4B, no significant differences were observed between groups C and D.
Note: Asterisk (*) indicates statistical significance at p<0.05
Abbreviations: ADT: Androgen deprivation therapy; a.u.: Arbitrary units; EIF4B: Eukaryotic translation initiation factor 4B; GAPDH: Glyceraldehyde-3-phosphate dehydrogenase; MID1: Midline 1; p-EIF4B: Phosphorylated eukaryotic translation initiation factor 4B; PIM2: Proviral integration site for Moloney murine leukemia virus 2; PP2A: Protein phosphatase 2A; XIAP: X-linked inhibitor of apoptosis protein.

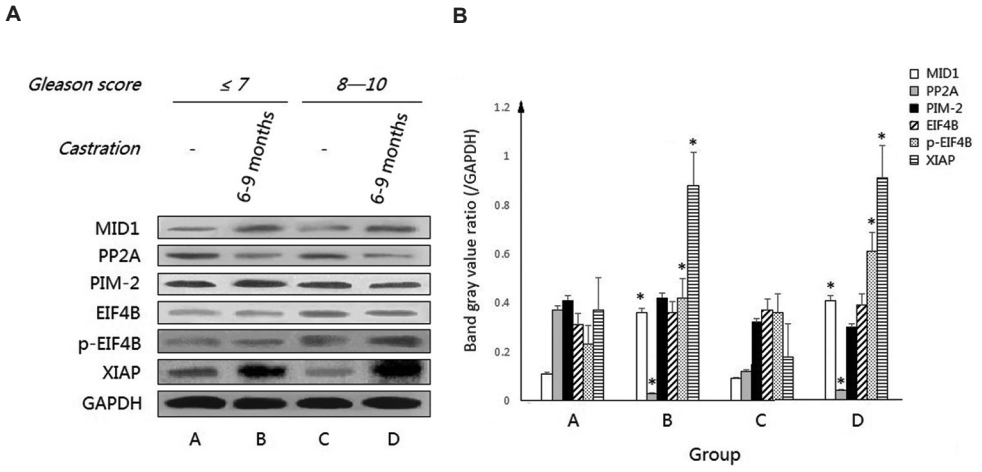

Figure 5. Expression of target proteins in patients with prostate cancer receiving 6–9 months of neoadjuvant ADT (group C; n = 13). (A) Western blot results; (B) Quantification of protein expression levels based on the band intensity ratio of each target protein to GAPDH. In patients with a Gleason score ≤7 (n = 8), XIAP protein expression levels were 0.370 ± 0.134 a.u. before ADT (group A) and 0.881 ± 0.137 a.u. after ADT (group B), demonstrating a statistically significant difference between groups A and B. p-EIF4B protein expression levels were 0.234 ± 0.082 a.u. before ADT (group A) and 0.422 ± 0.091 a.u. after ADT (group B), indicating a statistically significant difference between groups A and B. The protein expression levels of MID1 were 0.113 ± 0.010 a.u. before ADT (group A) and 0.361 ± 0.021 a.u. after ADT (group B), demonstrating a statistically significant difference between groups A and B. The protein expression levels of PP2A were 0.372 ± 0.019 a.u. before ADT (group A) and 0.032 ± 0.006 a.u. after ADT (group B), indicating a statistically significant difference between groups A and B. For PIM2 and EIF4B, no significant differences were observed between groups A and B. In patients with a Gleason score of 8–10 (n = 5), similar trends were observed in the protein expression levels of XIAP, p-EIF4B, PIM2, EIF4B, MID1, and PP2A before and after ADT (group C vs. group D).
Note: Asterisk (*) indicates statistical significance at p<0.05.
Abbreviations: ADT: Androgen deprivation therapy; a.u.: Arbitrary units; EIF4B: Eukaryotic translation initiation factor 4B; GAPDH: Glyceraldehyde-3-phosphate dehydrogenase; MID1: Midline 1; p-EIF4B: Phosphorylated eukaryotic translation initiation factor 4B; PIM2: Proviral integration site for Moloney murine leukemia virus 2; PP2A: Protein phosphatase 2A; XIAP: X-linked inhibitor of apoptosis protein.

3.3. MID1 modulates XIAP expression and apoptosis rate in prostate cancer cells

As an androgen-dependent prostate cancer cell line, LNCaP is typically regarded as a model of HSPC, whereas the androgen-independent PC-3 cell line is generally treated as a model of CRPC. In this study, LNCaP and PC-3 cells were employed to represent HSPC and CRPC, respectively, and to compare the protein expression levels of target factors between these two cell types.

Compared with the levels observed in LNCaP cells before castration, no significant differences were observed in the protein expression levels of XIAP, p-EIF4B, PIM2, EIF4B, MID1, and PP2A after castration for 4 or 8 weeks. However, after 16 weeks of castration, XIAP and p-EIF4B

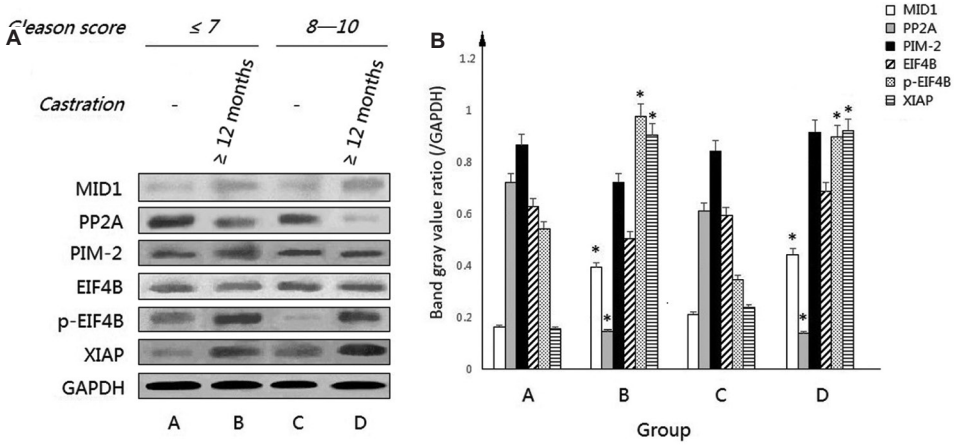

Figure 6. Expression of target proteins in patients with prostate cancer cases receiving no <12 months of neoadjuvant ADT (group D; $n = 9$). (A) Western blot results; (B) Quantification of protein expression levels based on the band intensity ratio of each target protein to GAPDH. For all cases, regardless of Gleason score, significant differences were observed in the protein expression levels of XIAP, p-EIF4B, MID1, and PP2A before and after ADT, showing a similar trend to that observed in group C. In contrast, no significant differences were found in the protein expression levels of PIM2 and EIF4B before and after ADT.

Note: Asterisk (*) indicates statistical significance at $p<0.05$.

Abbreviations: ADT: Androgen deprivation therapy; EIF4B: Eukaryotic translation initiation factor 4B; GAPDH: Glyceraldehyde-3-phosphate dehydrogenase; MID1: Midline 1; p-EIF4B: Phosphorylated eukaryotic translation initiation factor 4B; PIM2: Proviral integration site for Moloney murine leukemia virus 2; PP2A: Protein phosphatase 2A; XIAP: X-linked inhibitor of apoptosis protein.

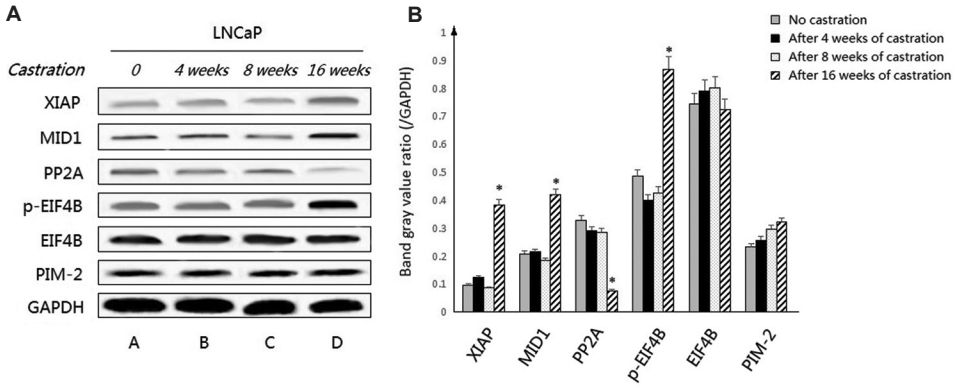

Figure 7. Expression of target proteins in LNCaP cells following different durations of castration ($n = 3$). (A) Western blot results; (B) Quantification of protein expression levels based on the band intensity ratio of each target protein to GAPDH. No significant differences were observed in the protein expression levels of XIAP, p-EIF4B, PIM2, EIF4B, MID1, and PP2A after 4 or 8 weeks of castration compared to baseline levels. However, after 16 weeks of castration, XIAP protein expression level increased significantly to 0.383 ± 0.017 a.u. Similarly, p-EIF4B and MID1 protein expression levels increased to 0.869 ± 0.046 a.u. and 0.419 ± 0.081 a.u., respectively. In contrast, PP2A expression levels significantly decreased to 0.076 ± 0.008 a.u. The expression levels of both PIM2 and EIF4B remained unchanged throughout the castration period.

Note: Asterisk (*) indicates statistical significance at $p<0.05$.

Abbreviations: a.u.: Arbitrary units; EIF4B: Eukaryotic translation initiation factor 4B; GAPDH: Glyceraldehyde-3-phosphate dehydrogenase; MID1: Midline 1; p-EIF4B: Phosphorylated eukaryotic translation initiation factor 4B; PIM2: Proviral integration site for Moloney murine leukemia virus 2; PP2A: Protein phosphatase 2A; XIAP: X-linked inhibitor of apoptosis protein.

levels were significantly increased. MID1 expression was also significantly elevated, whereas PP2A expression was significantly decreased. The protein expression levels of both PIM2 and EIF4B demonstrated no significant changes (Figure 7).

In LNCaP cells, both PIM2 and EIF4B protein expression levels remained unchanged following *MID1* transfection. However, PP2A protein expression level was significantly lower after *MID1* transfection. Both p-EIF4B and XIAP protein expression levels were significantly elevated after *MID1* transfection. Correspondingly, the apoptosis rate of LNCaP/MID1 cells was significantly lower than that of parental LNCaP cells (Figures 8 and 9).

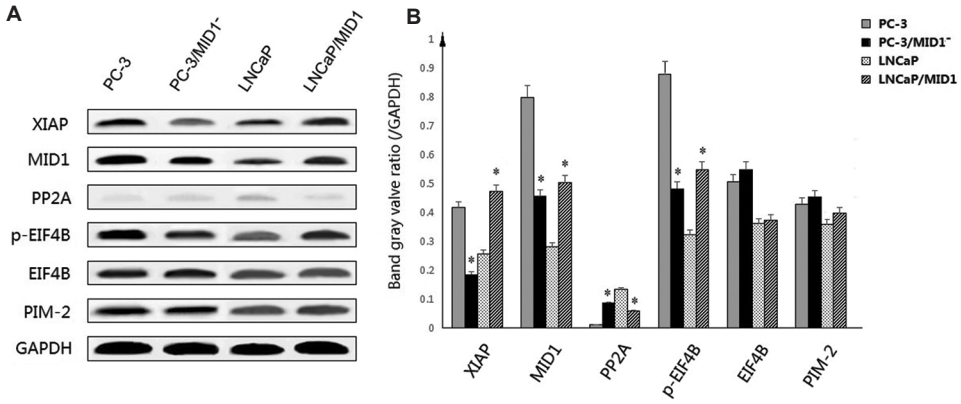

Figure 8. Expression of target proteins in PC-3 and LNCaP cells before and after *MID1* transfection (n = 3). (A) Western blot results; (B) Quantification of protein expression levels based on the band intensity ratio of each target protein to GAPDH. When *MID1* siRNA was transfected into PC-3 cells, the expression levels of MID1, p-EIF4B, and XIAP significantly decreased to 0.455 ± 0.031 a.u., 0.482 ± 0.021 a.u., and 0.185 ± 0.014 a.u., respectively. However, PP2A levels significantly increased to 0.086 ± 0.002 a.u. No significant differences were observed in PIM2 and EIF4B expression levels after transfection. When the *MID1* gene was transfected into LNCaP cells, the protein expression levels of MID1, p-EIF4B, and XIAP significantly increased to 0.503 ± 0.032 a.u., 0.548 ± 0.031 a.u., and 0.472 ± 0.027 a.u., respectively. In contrast, PP2A levels significantly decreased to 0.058 ± 0.001 a.u. No significant differences were observed in PIM2 and EIF4B levels after transfection.
Note: Asterisk (*) indicates statistical significance at p<0.05.
Abbreviations: a.u.: Arbitrary units; EIF4B: Eukaryotic translation initiation factor 4B; GAPDH: Glyceraldehyde-3-phosphate dehydrogenase; MID1: Midline 1; p-EIF4B: Phosphorylated eukaryotic translation initiation factor 4B; PIM2: Proviral integration site for Moloney murine leukemia virus 2; PP2A: Protein phosphatase 2A; XIAP: X-linked inhibitor of apoptosis protein.

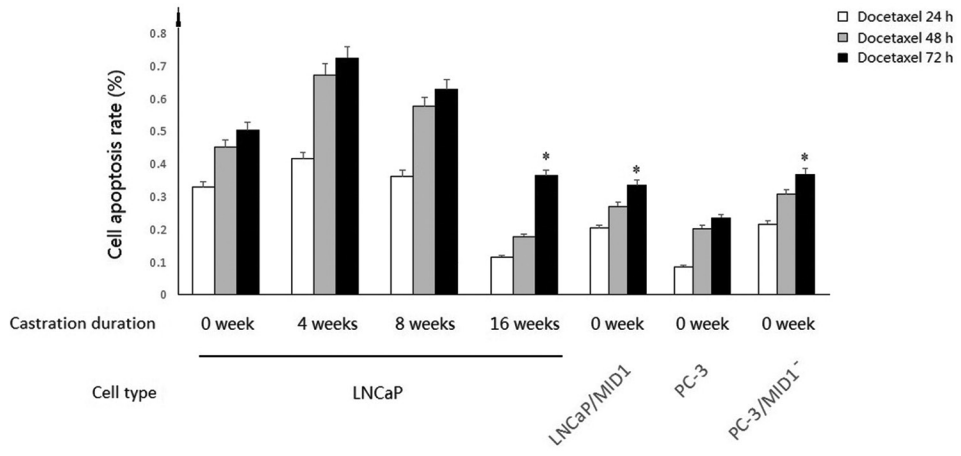

Figure 9. The apoptosis rate of different cell types (n = 3). The apoptosis rate increased in all cell types with prolonged docetaxel treatment and plateaued after 72 h. In LNCaP cells, a slight increase in apoptosis was observed after 4 and 8 weeks of castration compared to those without castration. However, after 16 weeks, the apoptosis rate significantly decreased relative to non-castrated LNCaP cells. In addition, LNCaP/MID1 cells exhibited a significantly lower apoptosis rate compared to LNCaP cells without castration. Although PC-3 cells showed a lower apoptosis rate than LNCaP cells, silencing MID1 expression significantly increased apoptosis in PC-3 cells.
Note: Asterisk (*) indicates statistical significance at p<0.05.9*+
Abbreviation: MID1: Midline 1.

In PC-3 cells, PIM2 and EIF4B protein expression levels remained unchanged following *MID1* siRNA transfection. However, PP2A protein expression level was significantly higher after the transfection of *MID1* siRNA. Both p-EIF4B and XIAP levels were significantly lower after *MID1* siRNA transfection compared to baseline levels. Consistently, the apoptosis rate of PC-3/MID1 siRNA cells was significantly higher than that of parental PC-3 cells (Figures 8 and 9).

4. Discussion

The majority of HSPC cases respond effectively to ADT, which has also led to a certain degree of overuse of ADT in clinical practice. For example, for patients with positive resection margins or positive lymph nodes following radical surgery, or those with high-risk factors such as high Gleason scores, clinicians may administer ADT indiscriminately in an effort to achieve optimal PSA outcomes. While this may result in better PSA control in the short term, it may also increase the likelihood or accelerate the onset of castration resistance in the long term, ultimately compromising overall survival benefits. This has become a recognized concern in clinical practice. Accordingly, investigating the relationship between ADT and the development of castration resistance holds significant clinical value.

PP2A is a major serine/threonine protein phosphatase in eukaryotic cells. It regulates substrate activity by dephosphorylating serine/threonine residues, thereby counteracting the effects of serine/threonine kinases. Studies have found that PP2A is involved in the regulation of multiple signaling pathways through its dephosphorylation activity. It has been reported that PP2A not only blocks cell proliferation pathways mediated by the MAPK/ERK and PI3K/AKT kinases[11] but also promotes the dephosphorylation and inactivation of cyclin CDC-25, thereby inhibiting cell cycle progression from the G2 phase to M phase and promoting apoptosis.[12] PP2A can also stabilize the tumor suppressor protein p53 through dephosphorylation, thereby enhancing p53-dependent apoptosis.[13] Therefore, PP2A has been widely studied as a tumor suppressor. Conversely, inhibition of PP2A activity may promote cell proliferation and facilitate tumorigenesis. Recent studies have shown that PP2A activity is significantly reduced in colon cancer and breast cancer cells, and that the PP2A agonist FTY720 can induce apoptosis in colon cancer and other malignant tumor cells.[14,15] PP2A is a heterotrimeric enzyme composed of three subunits: the structural subunit A, the regulatory subunit B, and the catalytic subunit C. The A and C subunits form the core enzyme, which is responsible for the catalytic activity of dephosphorylation, whereas the B subunit determines substrate specificity. Due to the presence of multiple B subunit isoforms with low sequence homology across different cell types, the substrate specificity of PP2A exhibits substantial cellular diversity.[16]

Previous research in liver cancer cells has shown that the B subunit of PP2A can recognize EIF4B via the conserved "RXRHXS" sequence located upstream of the phosphorylation site Ser422, subsequently dephosphorylating EIF4B at this site.[17] Notably, this site corresponds to the phosphorylation site targeted by PIM2 in prostate cancer cells.[4] In addition, previous studies have reported a lack of expression of the B subunit isoform PP2R2A in advanced prostate cancer cells,[18] suggesting that the activity of PP2A may be suppressed in advanced stages of the disease. These findings support the hypothesis that PP2A and PIM2 may competitively bind to EIF4B at Ser422, thereby co-regulating its phosphorylation status. Under physiological conditions, PP2A counteracts PIM2-mediated phosphorylation, thereby suppressing EIF4B overexpression and inhibiting XIAP-mediated anti-apoptotic activity. However, when PP2A expression is diminished or its activity is inhibited, its antagonistic effect on PIM2 is weakened. This functional imbalance may lead to an increased phosphorylation level of EIF4B despite unchanged PIM2 activity, thereby enhancing XIAP expression and promoting anti-apoptotic signaling. This hypothesis is consistent with the findings of the present study.

Microtubule-associated protein MID1 is a member of the tripartite motif family in eukaryotic cells, functioning as an E3 ubiquitin ligase that catalyzes the ubiquitination and subsequent degradation of specific substrates. MID1 interacts with the catalytic subunit C of PP2A (PP2Ac) to form a complex that promotes the ubiquitin-mediated degradation of PP2Ac.[19] Therefore, MID1 may contribute to the regulation of cell proliferation and tumorigenesis by downregulating PP2A activity.[20]

Previous research has shown that MID1 is highly expressed in prostate cancer cells – particularly in tumors with high Gleason scores and lymph node metastasis – suggesting that MID1 overexpression may be associated with poor prognosis in prostate cancer.[21] MID1 expression is negatively regulated by the AR signaling pathway and is inhibited when androgen binds to AR. However, in androgen-deficient environments, MID1 expression is markedly upregulated, thereby initiating downstream anti-apoptotic mechanisms. Since ADT induces an androgen-deficient state *in vivo*, it may trigger activation of the MID1/PP2A/EIF4B/XIAP pathway, thereby enhancing anti-apoptotic signaling. Consequently, prolonged ADT may facilitate the progression of prostate cancer toward a castration-resistant state.

This study provides a preliminary and limited investigation into the mechanism by which ADT induces castration resistance in prostate cancer cells through the regulation of XIAP expression. The primary focus was on protein detection in tissues and cells using Western blot analysis, a method that presents certain limitations. To strengthen these findings, further studies are warranted that incorporate gene knockout models and enzyme-linked immunosorbent assay, as well as a more in-depth exploration of the co-regulatory mechanism of EIF4B phosphorylation by PP2A and PIM2. In addition, the invasive and tumorigenic potential of cells subjected to gene transfection or gene knockout should be evaluated, which may provide a foundation for identifying potential therapeutic targets within this signaling pathway.

5. Conclusion

ADT may lead to elevated MID1 and reduced PP2A protein expression, which indirectly enhances PIM2-mediated phosphorylation of EIF4B. This, in turn, increases XIAP expression and reduces apoptosis in prostate cancer cells, ultimately promoting the progression to the castration-resistant stage.

Acknowledgments

None.

Funding

This research was supported by the Natural Science Foundation of Chongqing (cstc2021jcyj-msxmX0122; cstc2016jcjA0099) and the Natural Science Foundation of China (No. 81101945).

Conflict of interest

The authors declare that they have no competing interests.

Author contributions

Conceptualization: Ke Ren
Formal analysis: Xin Gou
Investigation: All authors
Methodology: Ke Ren
Writing – original draft: Ke Ren
Writing – review & editing: Xin Gou, Weiyang He

Ethics approval and consent to participate

The collection of all samples was conducted with the informed consent of the patients and their legal guardians. All procedures were approved by the Ethical Committee of Human Experimentation at the First Affiliated Hospital of Chongqing Medical University and were performed in accordance with the Declaration of Helsinki (1975).

Consent for publication

Not applicable.

Availability of data

Not applicable.

References

1. Chandrasekar T, Yang JC, Gao AC, Evans CP. Mechanisms of resistance in castration-resistant prostate cancer (CRPC). *Transl Androl Urol*. 2015;4:365-380.

   doi: 10.3978/j.issn.2223-4683.2015.05.02

2. Perera M, Roberts MJ, Klotz L, *et al*. Intermittent versus continuous androgen deprivation therapy for advanced prostate cancer. *Nat Rev Urol*. 2020;17(8):469-481.

   doi: 10.1038/s41585-020-0335-7

3. Ku JY, Lee JZ, Ha HK. The effect of continuous androgen deprivation treatment on prostate cancer patients as compared with intermittent androgen deprivation treatment. *Korean J Urol*. 2015;56(10):689-694.

   doi: 10.4111/kju.2015.56.10.689

4. Ren K, Gou X, Xiao M, *et al*. The over-expression of Pim-2 promote the tumorigenesis of prostatic carcinoma through phosphorylating eIF4B. *Prostate*. 2013;73(13):1462-1469.

   doi: 10.1002/pros.22693

5. Ren K, Gou X, Xiao M, He W, Kang J. Pim-2 cooperates with downstream factor XIAP to inhibit apoptosis and intensify malignant grade in prostate cancer. *Pathol Oncol Res*. 2019;25(1):341-348.

   doi: 10.1007/s12253-017-0353-9

6. Obexer P, Ausserlechner MJ. X-linked inhibitor of apoptosis protein - a critical death resistance regulator and therapeutic target for personalized cancer therapy. *Front Oncol*. 2014 28;4:197.

   doi: 10.3389/fonc.2014.00197

7. Ayachi O, Barlin M, Broxtermann PN, Kashkar H, Mauch C, Zigrino P. The X-linked inhibitor of apoptosis protein (XIAP) is involved in melanoma invasion by regulating cell migration and survival. *Cell Oncol (Dordr)*. 2019;42(3):319-329.

   doi: 10.1007/s13402-019-00427-1

8. Evans MK, Brown MC, Geradts J, *et al*. XIAP regulation by MNK links MAPK and NFκB signaling to determine an aggressive breast cancer phenotype. *Cancer Res*. 2018;78(7):1726-1738.

   doi: 10.1158/0008-5472.CAN-17-1667

9. Coyle R, Slattery K, Ennis L, O'sullivan MJ, Zisterer DM. The XIAP inhibitor embelin sensitises malignant rhabdoid tumour cells to TRAIL treatment via enhanced activation of the extrinsic apoptotic pathway. *Int J Oncol*. 2019;55(1):191-202.

doi: 10.3892/ijo.2019.4804

10. Lunardi A, Ala U, Epping MT, *et al*. A co-clinical approach identifies mechanisms and potential therapies for androgen deprivation resistance in prostate cancer. *Nat Genet*. 2013;45(7):747-755.

    doi: 10.1038/ng.2650

11. Zhang Q, Claret FX. Phosphatases: The new brakes for cancer development? *Enzyme Res*. 2012;2012:659649.

    doi: 10.1155/2012/659649

12. Alvarez-Fernández M, Halim VA, Aprelia M, Laoukili J, Mohammed S, Medema RH. Protein phosphatase 2A (B55α) prevents premature activation of forkhead transcription factor FoxM1 by antagonizing cyclin A/cyclin-dependent kinase-mediated phosphorylation. *J Biol Chem*. 2011;286(38):33029-33036.

    doi: 10.1074/jbc.M111.253724

13. Jin Z, Wallace L, Harper SQ, Yang J. PP2A: B56{epsilon}, a substrate of caspase-3, regulates p53-dependent and p53-independent apoptosis during development. *J Biol Chem*. 2010;285(45):34493-34502.

    doi: 10.1074/jbc.M110.169581

14. Baldacchino S, Saliba C, Petroni V, Fenech AG, Borg N, Grech G. Deregulation of the phosphatase, PP2A is a common event in breast cancer, predicting sensitivity to FTY720. *EPMA J*. 2014;5(1):3.

    doi: 10.1186/1878-5085-5-3

15. Cristóbal I, Manso R, Rincón R, *et al*. PP2A inhibition is a common event in colorectal cancer and its restoration using FTY720 shows promising therapeutic potential. *Mol Cancer Ther*. 2014;13(4):938-947.

    doi: 10.1158/1535-7163.MCT-13-0150

16. Grech G, Baldacchino S, Saliba C, *et al*. Deregulation of the protein phosphatase 2A, PP2A in cancer: Complexity and therapeutic options. *Tumour Biol*. 2016;37(9):11691-11700.

    doi: 10.1007/s13277-016-5145-4

17. Xu J, Lu Y, Liu Q, *et al*. Long noncoding RNA GMAN promotes hepatocellular carcinoma progression by interacting with eIF4B. *Cancer Lett*. 2020;473:1-12.

    doi: 10.1016/j.canlet.2019.12.032

18. Zhao Z, Kurimchak A, Nikonova AS, *et al*. PPP2R2A prostate cancer haploinsufficiency is associated with worse prognosis and a high vulnerability to B55α/PP2A reconstitution that triggers centrosome destabilization. *Oncogenesis*. 2019;8(12):72.

    doi: 10.1038/s41389-019-0180-9

19. Collison AM, Li J, De Siqueira AP, *et al*. TRAIL signals through the ubiquitin ligase MID1 to promote pulmonary fibrosis. *BMC Pulm Med*. 2019;19(1):31.

    doi: 10.1186/s12890-019-0786-x

20. Baldini R, Mascaro M, Meroni G. The MID1 gene product in physiology and disease. *Gene*. 2020;747:144655.

    doi: 10.1016/j.gene.2020.144655

21. Köhler A, Demir U, Kickstein E, *et al*. A hormone-dependent feedback-loop controls androgen receptor levels by limiting MID1, a novel translation enhancer and promoter of oncogenic signaling. *Mol Cancer*. 2014;13:146.

    doi: 10.1186/1476-4598-13-146